



Syntheses, characterization and electrocatalytical comparison of two cadmium-containing mono-lacunary Wells–Dawson polyoxometalates, α_1 - and α_2 -[P₂W₁₇Cd(H₂O)O₆₁]⁸⁻

FARROKHZAD MOHAMMADI ZONOZ^{1*}, ALI JAMSHIDI², FATEME HAJIZADEH¹ and KHADIJEH YOUSEFI³

¹Department of Chemistry, Hakim Sabzevari University, Sabzevar, 96179-76487, Iran,

²School of Chemistry, Damghan University, Damghan, Iran and ³Payamnoor University of Sari, Sari, Iran

(Received 18 January, revised 18 May, accepted 28 May 2014)

Abstract: Two new cadmium-containing Wells–Dawson polyoxometalates K₈[α_1 -P₂W₁₇Cd(H₂O)O₆₁]⁸⁻·14H₂O (α_1 -P₂W₁₇Cd) and K₈[α_2 -P₂W₁₇Cd(H₂O)O₆₁]⁸⁻·16H₂O (α_2 -P₂W₁₇Cd) were synthesized as water-soluble potassium salts. The cadmium-substituted complexes were characterized by IR, ³¹P-NMR, ¹¹³Cd-NMR spectroscopy and cyclic voltammetry (CV). Redox activities for the tungsten and cadmium centers were observed by cyclic voltammetry. It was found that the presence of cadmium decreased the electrocatalytic activity of the [α_1 -LiP₂W₁₇O₆₁]⁹⁻ and α_2 -[P₂W₁₇O₆₁]¹⁰⁻ heteropolyanions.

Keywords: polyoxometalates; Wells–Dawson; electrocatalytic; cadmium; cyclic voltammetry.

INTRODUCTION

Polyoxometalates (POMs), as a rich class of inorganic metal oxide cluster compounds, have different applications in molecular materials,¹ medicine, biology^{2,3} and catalysis^{4,5} due to their molecular, structural, and electronic versatility. The Dawson-type heteropolyanions with highly symmetric structures are famous as one kind of POMs. Their formula is [X₂W₁₈O₆₂]ⁿ⁻, where X is a heteroatom such as phosphorus.⁶ Removal of a WO unit from a cap WO₆ polyhedron of the (α -P₂W₁₈O₆₂)⁶⁻ (Wells–Dawson structure) results in the lacunary (α_2 -P₂W₁₇O₆₁)¹⁰⁻ isomer that has C_s symmetry, and removal of a WO unit from a belt WO₆ polyhedron results in the lacunary (α_1 -P₂W₁₇O₆₁)¹⁰⁻ isomer, that has C₁ symmetry (Fig. 1).^{7,8} An important structural characteristic of Dawson-type heteropolyanions is the possibility of replacing one of the tungsten atoms by a

*Corresponding author. E-mail: f.zonoz@hsu.ac.ir; fz.mohamadi@yahoo.com
doi: 10.2298/JSC140118057Z

transition metal cation, which possesses five bridging oxygens and a sixth oxo-group, which is occupied by a water molecule. For instance, transition metal *mono*-substituted Dawson anions with the general formula $K_8[\alpha_2\text{-P}_2\text{W}_{17}\text{M}\text{-(H}_2\text{O)}\text{O}_{61}]$ ($\text{M} = \text{Zr(IV), Hf(IV), Mn(II), Zn(II), Fe(II), Co(II), Cu(II) or Ni(II)}$) were investigated.^{9,10} Furthermore, these compounds have also been used as heterogeneous catalysts.^{11–13}

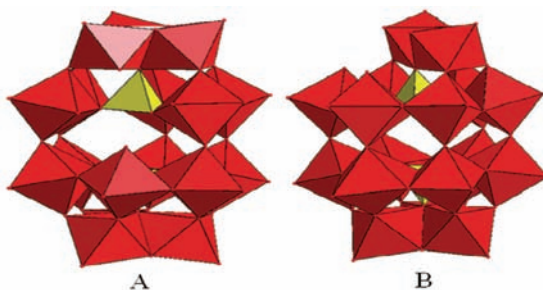


Fig. 1. A) The monovacant $\alpha_1\text{-[LiP}_2\text{W}_{17}\text{O}_{61}]^{9-}$ unit obtained by removing a WO_6 octahedron in the equatorial site of the parent Wells–Dawson structure, B) The monovacant $\alpha_2\text{-[P}_2\text{W}_{17}\text{O}_{61}]^{10-}$ unit obtained by removing a WO_6 octahedron in the capping region of the parent Wells–Dawson structure.

Until now, only a few cadmium-containing polyoxometalates have been reported. The first cadmium-containing heteropolyanions, related to the mono-lacunar anion of the Keggin structure (XW11) were presented by Contant.¹⁴ In 1995, Kirby and Baker¹⁵ reported the first sandwich-type heteropolyanions including Cd^{2+} based on the $[\text{P}_2\text{W}_{15}\text{O}_{56}]^{12-}$ defect structure, and later Bi *et al.*¹⁶ prepared a series of dimeric polytungstates by reacting $[\text{As}_2\text{W}_{15}\text{O}_{56}]^{12-}$ with M^{2+} ($\text{M} = \text{Cu(II), Mn(II), Co(II), Ni(II), Zn(II) or Cd(II)}$). Subsequently, Alizadeh *et al.*¹⁷ synthesized and structurally characterized $[\text{Cd}_4(\text{H}_2\text{O})_2(\text{PW}_9\text{O}_{34})_2]^{10-}$. In 2005, Kortz *et al.*¹⁸ reported another cadmium containing polyoxometalate, $[\text{Cd}_4\text{Cl}_2(B\text{-}\alpha\text{-AsW}_9\text{O}_{34})_2]^{12-}$. Finally, Zhao *et al.*¹⁹ prepared and characterized $[\text{Cd}_4(\text{H}_2\text{O})_2(B\text{-}\alpha\text{-SiW}_9\text{O}_{34})_2]^{12-}$.

Over past years, electrochemical methods were shown to be an inexpensive and effective method for the determination of some inorganic and organic substrates.^{20–23} In particular, POMs exhibited multi-electron reversible redox characteristics, which enables them to be redox electrocatalysts for some irreversible electrochemical processes.^{24–26} In electrochemistry, the main processes include the reduction of protons or the oxidation of hydrogen, the reduction of dioxygen, and the electrochemical processes of nitrogen oxides NO_x and carbon oxides CO_x , complemented by the electrocatalysis of bromate, iodate and so forth. All of these reactions have important implications in environmental problems and/or are potentially considered to be abundant, inexpensive sources for the production of useful chemicals.²⁷ In this paper, the syntheses of two new cadmium-containing

α_1 - and α_2 -mono-lacunary Dawson-type polyoxometalates, $K_8[\alpha_1\text{-P}_2\text{W}_{17}\text{Cd}(\text{H}_2\text{O})\text{O}_{61}]\cdot14\text{H}_2\text{O}$ ($\alpha_1\text{-P}_2\text{W}_{17}\text{Cd}$) and $K_8[\alpha_2\text{-P}_2\text{W}_{17}\text{Cd}(\text{H}_2\text{O})\text{O}_{61}]\cdot16\text{H}_2\text{O}$ ($\alpha_2\text{-P}_2\text{W}_{17}\text{Cd}$), are described. Several attempts to prepare single crystals of $\alpha_1\text{-P}_2\text{W}_{17}\text{Cd}$ and $\alpha_2\text{-P}_2\text{W}_{17}\text{Cd}$ failed. Therefore, these compounds were characterized by elemental analysis, and FT-IR, ^{31}P -NMR and ^{113}Cd -NMR spectroscopic methods. The electrochemical properties of these compounds and the electrocatalytic reductions of nitrite were investigated in detail by cyclic voltammetry.

EXPERIMENTAL

All reagents were of analytical grade and were used as received from commercial sources without further purification. The mono-lacunary POMs $K_{10}[\alpha_2\text{-P}_2\text{W}_{17}\text{O}_{61}]\cdot20\text{H}_2\text{O}$ and $K_9[\alpha_1\text{-LiP}_2\text{W}_{17}\text{O}_{61}]\cdot20\text{H}_2\text{O}$ were prepared according to the literature and characterized accordingly.²⁸ FT-IR spectra were recorded in the range 400–4000 cm⁻¹ on an Alpha Centaur FT-IR spectrophotometer using the KBr pellet technique. The NMR spectrum was recorded on a Bruker BRX-300 Avance spectrometer. The resonance frequencies for the ^{31}P and ^{113}Cd nuclei are at 202.46 and 110.92 MHz, respectively. The chemical shifts for the ^{31}P - and ^{113}Cd -NMR spectra were externally referenced relative to 85 % H_3PO_4 and 0.1 M cadmium perchlorate, respectively. Elemental analyses were realized using an Integra XL inductively coupled plasma spectrometer. The water used for all electrochemical measurements was obtained by passing through a Millipore Q water purification set. The solutions were deaerated thoroughly for at least 30 min by bubbling with pure N_2 and kept under N_2 atmosphere during the whole experiment. The electrochemical set-up was a Metrohm 797VA computrace polarographic analyzer. A conventional three-electrode system was used. The working electrode was a glassy carbon electrode. A platinum electrode was used as the counter electrode and an Ag/AgCl (3 M KCl) electrode was employed as the reference electrode. All potentials were measured and reported vs. the Ag/AgCl electrode. All voltammetric experiments were performed at room temperature.

Synthesis of $K_8[\alpha_1\text{-P}_2\text{W}_{17}\text{Cd}(\text{H}_2\text{O})\text{O}_{61}]\cdot14\text{H}_2\text{O}$

$\text{Cd}(\text{NO}_3)_2\cdot4\text{H}_2\text{O}$ (0.72 g, 2.33 mmol) was dissolved in 40 mL of sodium acetate buffer (0.25 M, pH 4.7). The solution was heated to 80 °C and then, 10 g (2.08 mmol) of $K_9[\alpha_1\text{-LiP}_2\text{W}_{17}\text{O}_{61}]\cdot20\text{H}_2\text{O}$ was added gradually. After 2 h, the solution was cooled to room temperature, and precipitate was removed by filtration. This solid was recrystallized from boiling water and dried under vacuum. Yield: 41.58 %; Anal. Calcd. for $\text{CdH}_{30}\text{K}_8\text{O}_{76}\text{P}_2\text{W}_{17}$: Cd, 2.31; K, 6.43; P, 1.27; W, 64.32; H_2O , 5.18 %. Found: Cd, 2.28; K, 6.30; P, 1.23; W, 64.35; H_2O , 5.24 %. IR (KBr, cm⁻¹): 1084, 1060, 1014 (P–O stretching bonds), 948 (W–O_{term} stretching bonds), 898 (W–O_b stretching bonds), 784, 738 (W–O_c stretching bonds).

Synthesis of $K_8[\alpha_2\text{-P}_2\text{W}_{17}\text{Cd}(\text{H}_2\text{O})\text{O}_{61}]\cdot16\text{H}_2\text{O}$

A 0.72 g (2.33 mmol) of $\text{Cd}(\text{NO}_3)_2\cdot4\text{H}_2\text{O}$ was dissolved in 40 mL of sodium acetate buffer (0.25 M, pH 4.7). The solution was heated to 90 °C and then 10 g (2.03 mmol) of $K_{10}[\alpha_2\text{-P}_2\text{W}_{17}\text{O}_{61}]\cdot20\text{H}_2\text{O}$ was added gradually. After 2 h, the solution was cooled to room temperature and precipitate was removed by filtration. This solid was recrystallized from boiling water and dried under vacuum. Yield: 61.4 %; Anal. Calcd. for $\text{CdH}_{34}\text{K}_8\text{O}_{78}\text{P}_2\text{W}_{17}$: Cd, 2.29; K, 6.39; P, 1.26; W, 63.85; H_2O , 5.88 %. Found: Cd, 2.24; K, 5.45; P, 1.16; W,

64.81; H₂O, 5.82 %. IR (KBr, cm⁻¹): 1085, 1053, 1016 (P–O stretching bonds), 945 (W–O_{term} stretching bonds), 889 (W–O_b stretching bonds), 800, 730 (W–O_c stretching bonds).

RESULTS AND DISCUSSION

IR spectra

The compounds $\alpha_1\text{-P}_2\text{W}_{17}\text{Cd}$ and $\alpha_2\text{-P}_2\text{W}_{17}\text{Cd}$, synthesized in this work, showed typical bands of transition metal-substituted Wells–Dawson heteropolyanion in the range of 700–1200 cm⁻¹.²⁹ The solid-state FT-IR measurements of K₆[$\alpha\text{-P}_2\text{W}_{18}\text{O}_{62}$]⁶⁻, K₉[$\alpha_1\text{-LiP}_2\text{W}_{17}\text{O}_{61}$]⁶⁻, $\alpha_1\text{-P}_2\text{W}_{17}\text{Cd}$, K₁₀[$\alpha_2\text{-P}_2\text{W}_{17}\text{O}_{61}$]⁶⁻ and $\alpha_2\text{-P}_2\text{W}_{17}\text{Cd}$ (Fig. 2, curves a–e, respectively) show the spectral patterns characteristic of the Dawson POM framework.

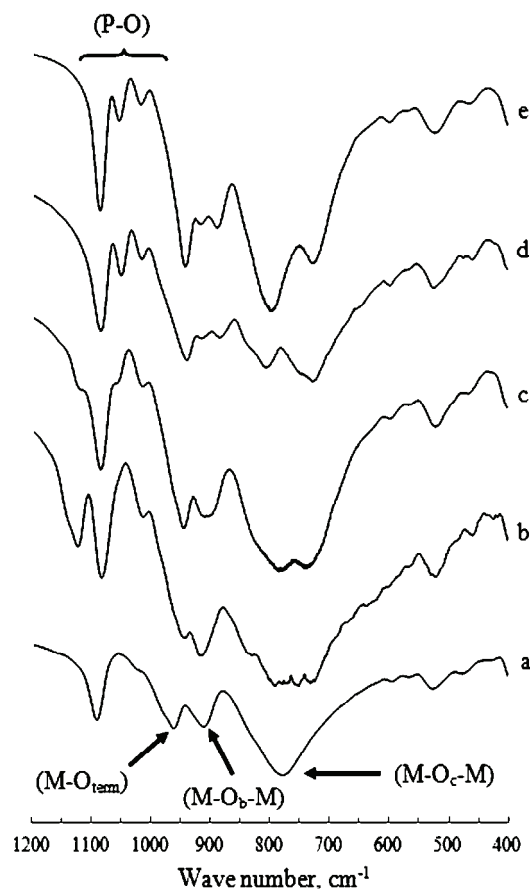


Fig. 2. IR spectra of: a) K₆[$\alpha\text{-P}_2\text{W}_{18}\text{O}_{62}$]⁶⁻; b) K₉[$\alpha_1\text{-LiP}_2\text{W}_{17}\text{O}_{61}$]⁶⁻; c) $\alpha_1\text{-P}_2\text{W}_{17}\text{Cd}$; d) K₁₀[$\alpha_2\text{-P}_2\text{W}_{17}\text{O}_{61}$]⁶⁻; e) $\alpha_2\text{-P}_2\text{W}_{17}\text{Cd}$.

As seen in Fig. 2, it is remarkable that only two bands of (P–O) stretching vibration were observed within the range of 1000–1200 cm⁻¹ in the [$\alpha\text{-P}_2\text{W}_{18}\text{O}_{62}$]⁶⁻ heteropolyanion,³⁰ whereas three bands were observed within the range of 1000–

-1200 cm^{-1} in the $[\alpha_1\text{-LiP}_2\text{W}_{17}\text{O}_{61}]^{9-}$ heteropolyanion. In $\alpha_1\text{-P}_2\text{W}_{17}\text{Cd}$, by replacing Cd^{2+} in the mono-lacunary $[\alpha_1\text{-LiP}_2\text{W}_{17}\text{O}_{61}]^{9-}$ polyoxometalate, significant changes were observed in the (P–O) stretching region. As seen in Fig. 2, curve c, the 1122 cm^{-1} band was observed as a shoulder and therefore, the pattern of the spectrum of $\alpha_1\text{-P}_2\text{W}_{17}\text{Cd}$ was approximately similar to that of $[\alpha_1\text{-P}_2\text{W}_{18}\text{O}_{62}]^{6-}$. It was surmised that removal of the bands was due to the increase in the symmetry of PO_4 unit caused by transition metal substitution.³¹ Moreover, the FT-IR spectra of $\alpha_1\text{-P}_2\text{W}_{17}\text{Cd}$ in the (M–O) region are very similar to that of $\text{K}_9[\alpha_1\text{-LiP}_2\text{W}_{17}\text{O}_{61}]$, especially with regards to the (M–O_{term}) oxygen atoms (948 cm^{-1} for $\alpha_1\text{-P}_2\text{W}_{17}\text{Cd}$ and 945 cm^{-1} for $\text{K}_9[\alpha_1\text{-LiP}_2\text{W}_{17}\text{O}_{61}]$), the bands assignable to corner-sharing (M–O_b–M) oxygen atoms (898 cm^{-1} for $\alpha_1\text{-P}_2\text{W}_{17}\text{Cd}$ and 912 cm^{-1} for $\text{K}_9[\alpha_1\text{-LiP}_2\text{W}_{17}\text{O}_{61}]$) and the bands assignable to edge-sharing (M–O_c–M) oxygen atoms (784 and 738 cm^{-1} for $\alpha_1\text{-P}_2\text{W}_{17}\text{Cd}$; 790 and 732 cm^{-1} for $\text{K}_9[\alpha_1\text{-LiP}_2\text{W}_{17}\text{O}_{61}]$). The FT-IR spectra of $\alpha_2\text{-P}_2\text{W}_{17}\text{Cd}$ in the polyoxometalate region were very similar to that of $\text{K}_{10}[\alpha_2\text{-P}_2\text{W}_{17}\text{O}_{61}]$, especially with regards to the multiple (P–O) bands (1085 , 1053 and 1016 cm^{-1} for $\alpha_2\text{-P}_2\text{W}_{17}\text{Cd}$; 1083 , 1047 , and 1016 cm^{-1} for $\text{K}_{10}[\alpha_2\text{-P}_2\text{W}_{17}\text{O}_{61}]$), the bands assignable to (M–O_{term}) oxygen atoms (943 cm^{-1} for $\alpha_2\text{-P}_2\text{W}_{17}\text{Cd}$ and 939 cm^{-1} for $\text{K}_{10}[\alpha_2\text{-P}_2\text{W}_{17}\text{O}_{61}]$), the bands assignable to corner-sharing (M–O_b–M) oxygen atoms (889 cm^{-1} for $\alpha_2\text{-P}_2\text{W}_{17}\text{Cd}$ and 885 cm^{-1} for $\text{K}_{10}[\alpha_2\text{-P}_2\text{W}_{17}\text{O}_{61}]$) and the bands assignable to edge-sharing (M–O_c–M) oxygen atoms (800 and 730 cm^{-1} for $\alpha_2\text{-P}_2\text{W}_{17}\text{Cd}$; 868 and 736 cm^{-1} for $\text{K}_{10}[\alpha_2\text{-P}_2\text{W}_{17}\text{O}_{61}]$).

³¹P-NMR

³¹P-NMR spectroscopy is a very sensitive technique to characterize polyoxometalates and evaluate the purity of these compounds. The ³¹P-NMR data obtained in this study work and the data for some transition-metal substituted Dawson-type polyoxometalates are given in Table I. In this table, P (1) refers to

TABLE I. ³¹P-NMR chemical shift patterns (δ / ppm) for some phosphotungstate Dawson-type polyoxometalates; P (1) refers to the resonance attributed to the phosphorus atom nearer to the site of substitution (or defect); P (2) refers to the P atom far away from the site of substitution (or defect)

Compound	P (1)	P (2)	Ref.
$\text{K}_6[\alpha\text{-P}_2\text{W}_{18}\text{O}_{62}]$	-12.50	-12.5	28
$\text{K}_9[\alpha_1\text{-LiP}_2\text{W}_{17}\text{O}_{61}]$	-9.00	-13.1	28
$\text{K}_{10}[\alpha_2\text{-P}_2\text{W}_{17}\text{O}_{61}]$	-6.90	-13.70	32
$\text{K}_8[\alpha_1\text{-P}_2\text{W}_{17}\text{Zn}(\text{H}_2\text{O})\text{O}_{61}]$	-8.56	-13.45	33
$\text{K}_8[\alpha_2\text{-P}_2\text{W}_{17}\text{Zn}(\text{H}_2\text{O})\text{O}_{61}]$	-8.65	-14.15	33
$\text{K}_7[\alpha_1\text{-P}_2\text{W}_{17}\text{La}(\text{H}_2\text{O})_4\text{O}_{61}]$	-10.58	-13.64	34
$\text{K}_7[\alpha_1\text{-P}_2\text{W}_{17}\text{Lu}(\text{H}_2\text{O})_4\text{O}_{61}]$	-10.57	-13.55	34
$\text{K}_7[\alpha_2\text{-P}_2\text{W}_{17}\text{Lu}(\text{H}_2\text{O})_4\text{O}_{61}]$	-10.58	-13.61	34
$\text{K}_8[\alpha_1\text{-P}_2\text{W}_{17}\text{Cd}(\text{H}_2\text{O})\text{O}_{61}]$	-7.99	-14.19	This work
$\text{K}_8[\alpha_2\text{-P}_2\text{W}_{17}\text{Cd}(\text{H}_2\text{O})\text{O}_{61}]$	-6.72	-13.00	This work

the resonance attributed to the P atom nearer to the site of substitution (or defect) and P (2) refers to the P atom far away from the site of substitution (or defect). In addition, ^{31}P -NMR spectra of $\alpha_1\text{-P}_2\text{W}_{17}\text{Cd}$ and $\alpha_2\text{-P}_2\text{W}_{17}\text{Cd}$ are shown in Fig. 3. The two-line ^{31}P -NMR spectra strongly suggest the presence of a single species in solution, thereby precluding the presence of even minor, phosphorus-containing impurities in $\alpha_1\text{-P}_2\text{W}_{17}\text{Cd}$ or $\alpha_2\text{-P}_2\text{W}_{17}\text{Cd}$. Finally, the integrated intensity of P (1) appears smaller than that of P (2) because of a slow relaxation rate (large T_1).

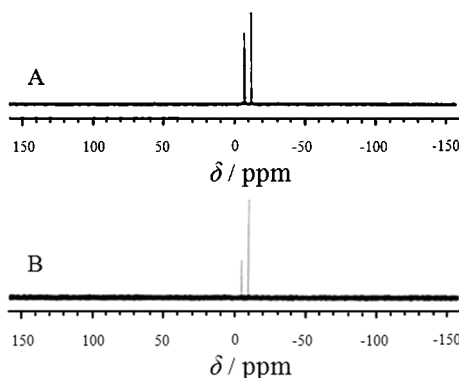


Fig. 3. ^{31}P -NMR spectra of A) $\alpha_1\text{-P}_2\text{W}_{17}\text{Cd}$ and B) $\alpha_2\text{-P}_2\text{W}_{17}\text{Cd}$.

^{113}Cd -NMR

The ^{113}Cd -NMR spectra in D_2O show clean, single spectra with a resonance at $\delta = 63.34$ ppm for $\alpha_1\text{-P}_2\text{W}_{17}\text{Cd}$ (Fig. 4A) and at $\delta = -22.86$ ppm for $\alpha_2\text{-P}_2\text{W}_{17}\text{Cd}$ (Fig. 4B). As shown in Fig. 4, a considerable difference was observed between the chemical shifts in the ^{113}Cd -NMR spectra of $\alpha_1\text{-P}_2\text{W}_{17}\text{Cd}$ and $\alpha_2\text{-P}_2\text{W}_{17}\text{Cd}$. Francesconi *et al.*³⁵ reported that the basic oxygen of the α_1 structure is bound to one tungsten atom, while the corresponding oxygen of the α_2 structure is bound to two tungsten atoms. This observation is ascribed mainly to

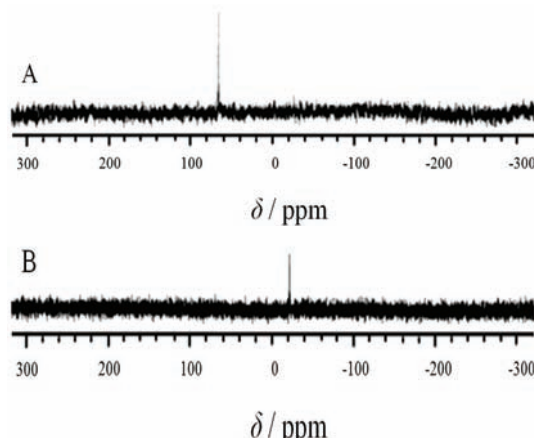


Fig. 4. ^{113}Cd -NMR spectra of A) $\alpha_1\text{-P}_2\text{W}_{17}\text{Cd}$ and B) $\alpha_2\text{-P}_2\text{W}_{17}\text{Cd}$.

the large framework distortion induced by the vacancy in the α_1 site, and to the nature of the cadmium substituent, which could be considered as not filling the vacancy completely and hence, its resonance moves to an upfield value. On the other hand, for the α_2 site, the cadmium substituent fills the vacancy perfectly and therefore its resonance is downfield shifted.

Electrochemical behavior of $\alpha_1\text{-P}_2\text{W}_{17}\text{Cd}$ and $\alpha_2\text{-P}_2\text{W}_{17}\text{Cd}$

Electrochemical behavior of $\alpha_1\text{-P}_2\text{W}_{17}\text{Cd}$. The electrochemical behavior of $\alpha_1\text{-P}_2\text{W}_{17}\text{Cd}$ was studied in 0.5 M acetate buffer solution by cyclic voltammetry (CV), and the obtained results are compared in Fig. 5 with those for $[\alpha_1\text{-LiP}_2\text{W}_{17}\text{O}_{61}]^{9-}$. As can be clearly seen in Fig. 5, four quasi-reversible redox peaks appeared in the potential range -1.1 to -0.3 V at a scan rate of 75 mV s^{-1} . The cathodic peak potentials were at -0.97 V (tungsten center), -0.84 V (tungsten center), -0.61 V (tungsten and cadmium centers) and -0.46 V (tungsten center) for $\alpha_1\text{-P}_2\text{W}_{17}\text{Cd}$ while the corresponding peaks were found at -0.97 , -0.7 , -0.6 and -0.43 V, respectively, for $[\alpha_1\text{-LiP}_2\text{W}_{17}\text{O}_{61}]^{9-}$. On considering these data, when cadmium replaced in polyoxometalate vacancy, the cadmium potential would be shifted toward negative potential and the current intensity at -0.6 V would be increased considerably, however the oxidation and reduction of Cd^{2+}/Cd , in the free ion state, occurs at -0.4 V.³⁶

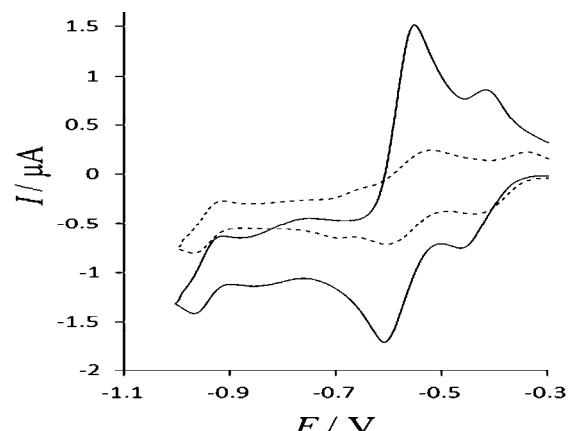


Fig. 5. Cyclic voltammograms of $\alpha_1\text{-P}_2\text{W}_{17}\text{Cd}$ (solid line) and $\text{K}_9[\alpha_1\text{-LiP}_2\text{W}_{17}\text{O}_{61}]$ (dashed line).

The cyclic voltammograms of $\alpha_1\text{-P}_2\text{W}_{17}\text{Cd}$ in 0.5 M acetate buffer solution at different scan rates are shown in Fig. 6. When the scan rate was varied from 25 to 750 mV s^{-1} , the cathodic peak potentials shifted in the negative direction and the corresponding anodic peak potentials shifted in the positive direction with increasing scan rate. The plots of peak (III) current vs. scan rate are shown in the inset of Fig. 6. At scan rates slower than 100 mV s^{-1} , the anodic currents were proportional to the square root of the scan rate, which indicates that the redox

process was diffusion-controlled; however, at scan rates higher than 100 mV/s, the anodic currents were proportional to the scan rate, suggesting that the redox process was surface-confined.

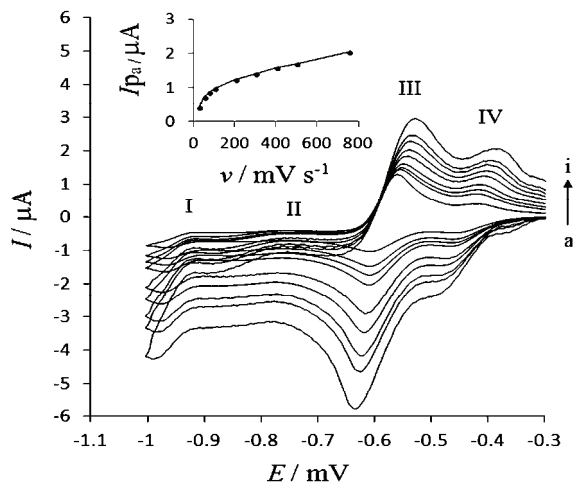


Fig. 6. Cyclic voltammograms of $\alpha_1\text{-P}_2\text{W}_{17}\text{Cd}$ in 0.5 M acetate buffer solutions at different scan rates of a) 25, b) 50, c) 75, d) 100, e) 200, f) 300, g) 400, h) 500 and i) 750 mV s^{-1} . The inset shows plots of the anodic peak current of III against scan rate.

Electrochemical behavior of $\alpha_2\text{-P}_2\text{W}_{17}\text{Cd}$. The electrochemical behavior of $\alpha_2\text{-P}_2\text{W}_{17}\text{Cd}$ was studied in 0.5 M acetate buffer solution by cyclic voltammetry (CV). The obtained results are compared with the corresponding results for $[\alpha_2\text{-P}_2\text{W}_{17}\text{O}_{61}]^{10-}$ in Fig. 7, from which it can be clearly seen that in the potential range -1.1 to -0.3 V, three quasi-reversible redox peaks appeared and the cathodic peak potentials for a scan rate of 75 mV s^{-1} were at -0.87 (tungsten center), -0.61 (tungsten and cadmium centers) and -0.47 V (tungsten center) for $\alpha_2\text{-P}_2\text{W}_{17}\text{Cd}$ and at -0.95 , -0.67 and -0.54 V, respectively, for $[\alpha_2\text{-P}_2\text{W}_{17}\text{O}_{61}]^{10-}$. Similar to $\alpha_1\text{-P}_2\text{W}_{17}\text{Cd}$, on substituting cadmium in the polyoxometalate vac-

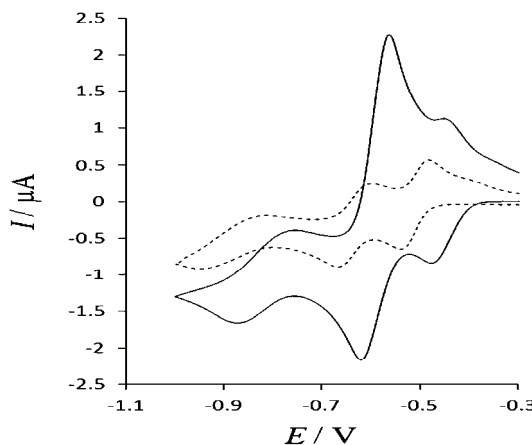


Fig. 7. Cyclic voltammograms of $\alpha_2\text{-P}_2\text{W}_{17}\text{Cd}$ (solid line) and $\text{K}_{10}[\alpha_2\text{-P}_2\text{W}_{17}\text{O}_{61}]$ (dashed line).

ancy, the cadmium potential was shifted toward negative potentials and the current intensity at -0.6 V increased considerably, although the oxidation and reduction of Cd^{2+}/Cd in the free ion state occurs at -0.4 V.³⁶

On comparison of cathodic potential data between $\alpha_1\text{-P}_2\text{W}_{17}\text{Cd}$ and $[\alpha_1\text{-LiP}_2\text{W}_{17}\text{O}_{61}]^{9-}$, and between $\alpha_2\text{-P}_2\text{W}_{17}\text{Cd}$ and $[\alpha_2\text{-P}_2\text{W}_{17}\text{O}_{61}]^{10-}$, it is obvious that when cadmium replaced the vacancy in $[\alpha_1\text{-LiP}_2\text{W}_{17}\text{O}_{61}]^{9-}$, no significant changes in the cathodic potentials for $\alpha_1\text{-P}_2\text{W}_{17}\text{Cd}$ were observed. However, when cadmium replaced the vacancy in $[\alpha_2\text{-P}_2\text{W}_{17}\text{O}_{61}]^{10-}$, considerable changes in these potentials were observed for $\alpha_2\text{-P}_2\text{W}_{17}\text{Cd}$. These results indicate that cadmium, which substituted completely in the $[\alpha_2\text{-P}_2\text{W}_{17}\text{O}_{61}]^{10-}$ vacancy affects the redox potentials of the tungsten centers of the polyoxometalate, while cadmium in $\alpha_1\text{-P}_2\text{W}_{17}\text{Cd}$ does not fill the vacancy of $[\alpha_1\text{-LiP}_2\text{W}_{17}\text{O}_{61}]^{9-}$ completely.

Figure 8 shows the cyclic voltammograms of $\alpha_2\text{-P}_2\text{W}_{17}\text{Cd}$ at different scan rates in the 0.5 M acetate buffer solution. When the scan rate was varied from 10 to 750 mV s $^{-1}$, the cathodic peak potentials were shifted in the negative direction and the corresponding anodic peak potentials shifted in the positive direction with increasing scan rate. The plots of peak (III) current vs. scan rate are shown in the inset of Fig. 8. At scan rates lower than 75 mV s $^{-1}$, the anodic currents were proportional to the square root of the scan rate, which indicates that the redox process was diffusion-controlled; however, at scan rates faster than 75 mV s $^{-1}$, the anodic currents were proportional to the scan rate, suggesting that the redox process is surface-confined.

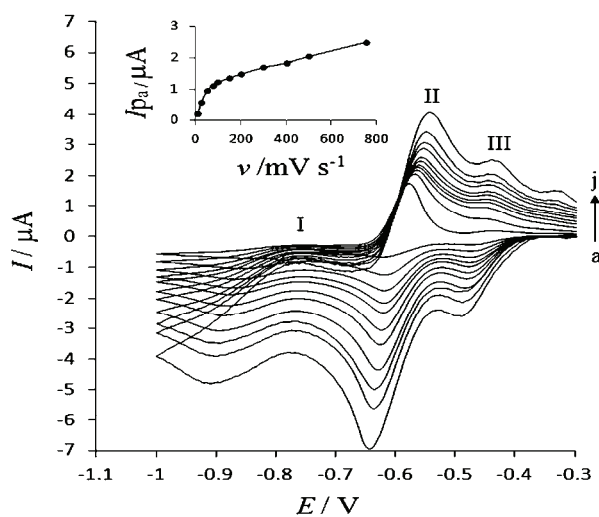


Fig. 8. Cyclic voltammograms of $\alpha_2\text{-P}_2\text{W}_{17}\text{Cd}$ in 0.5 M acetate buffer solutions at different scan rates of a) 10 , b) 25 , c) 50 , d) 75 , e) 100 , f) 200 , g) 300 , h) 400 , i) 500 and j) 750 mV s $^{-1}$.

The inset shows plots of the anodic peak current of III against scan rate.

Electrocatalysis of NO_2^- reduction

As is known, POMs have been exploited extensively in electrocatalytic reductions.³⁷ For example, Keita *et al.* reported the first examples of efficient participation of selected metal-ion-substituted heteropolyanions in the electrocatalytic reduction of nitrate and that vanadium-substituted Dawson-types are versatile electrocatalysts.^{38,39}

Electrocatalysis of NO_2^- reduction by $\alpha_1\text{-P}_2\text{W}_{17}\text{Cd}$

The polyoxometalates $[\alpha_1\text{-LiP}_2\text{W}_{17}\text{O}_{61}]^{9-}$ and $\alpha_1\text{-P}_2\text{W}_{17}\text{Cd}$ were tested at pH 4.7 for their activity in the reduction of nitrite ion. The CVs for the electrocatalytic reduction of NO_2^- by glassy carbon electrode in the 0.5 M acetate buffer solution are shown in Fig. 9.

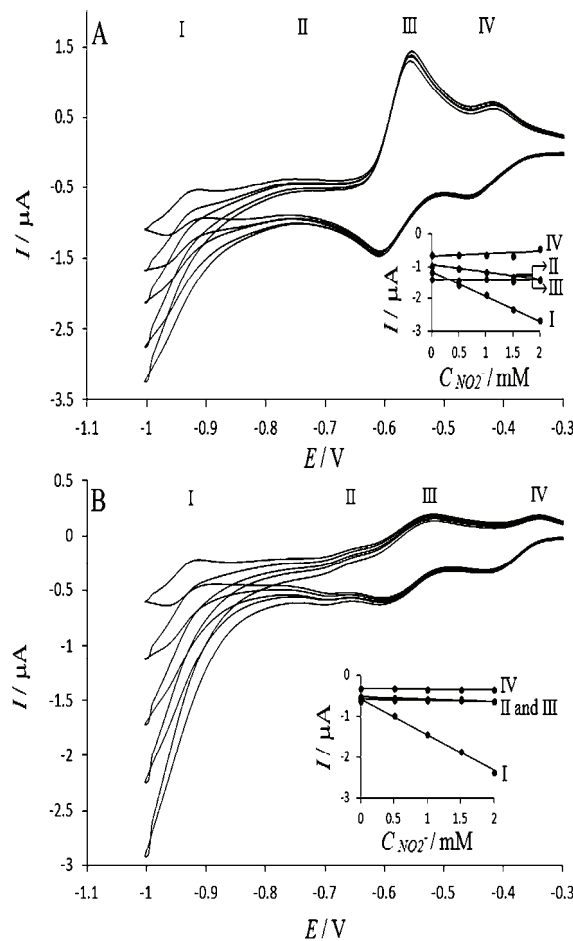


Fig. 9. A) Cyclic voltammograms (scan rate: 75 mV s^{-1}) for the electrocatalytic reduction of NO_2^- with a $5 \times 10^{-4} \text{ M}$ solution of $\alpha_1\text{-P}_2\text{W}_{17}\text{Cd}$ in a 0.5 M acetate buffer solution (from top to bottom $\gamma = 0, 1, 2, 3$ and 4). B) Cyclic voltammograms (scan rate: 75 mV s^{-1}) for the electrocatalytic reduction of NO_2^- with a $5 \times 10^{-4} \text{ M}$ solution of $\text{K}_9[\alpha_1\text{-LiP}_2\text{W}_{17}\text{O}_{61}]$ in a 0.5 M acetate buffer solution (from top to bottom $\gamma = 0, 1, 2, 3$ and 4). The excess parameter defined as $\gamma = c^0_{(\text{NO}_2^-)} / c^0_{(\text{POM})}$. Inset: the relationship between catalytic current and the NO_2^- concentration.

Clearly, with the addition of NaNO₂ to the solution, even for small values of the excess parameter, γ , which is defined here as:

$$\gamma = \frac{c_{(\text{NO}_x)}^0}{c_{(\text{POM})}^0}$$

the cathodic current of all waves increased and the corresponding anodic current decreased. The catalytic efficiency *CAT* for waves I and II of [α₁-LiP₂W₁₇O₆₁]⁹⁻ varied from 53.20 to 274.02 % and 4.53 to 19.84 %, respectively (Table II), when γ increase from 1 to 4, while the *CAT* for α₁-P₂W₁₇Cd varied from 34.74 to 127.9 % (wave I) and 9.26 to 43.6 % (wave II), Table III. *CAT* is defined as:

$$CAT = 100 \times \frac{[I_p(\text{POM}, \text{NaNO}_2) - I_p(\text{POM})]}{I_p(\text{POM})}$$

where $I_p(\text{POM})$ and $I_p(\text{POM}, \text{NaNO}_2)$ are the cathodic peak currents in the absence and in the presence of NaNO₂, respectively.

TABLE II. Catalytic efficiency for [α₁-LiP₂W₁₇O₆₁]⁹⁻; *CATw_x* refers to catalytic efficiency for the x^{th} wave

γ	<i>CATw₁</i> / %	<i>CATw₂</i> / %	<i>CATw₃</i> / %	<i>CATw₄</i> / %
1	53.20	4.53	2.80	3.52
2	123.78	10.39	6.84	8.01
3	191.07	11.34	5.78	6.73
4	274.02	19.84	10.87	1.21

TABLE III. Catalytic efficiency for α₁-P₂W₁₇Cd; *CATw_x* refers to catalytic efficiency for the x^{th} wave

γ	<i>CATw₁</i> / %	<i>CATw₂</i> / %	<i>CATw₃</i> / %	<i>CATw₄</i> / %
1	34.74	9.26	3.57	4.51
2	61.01	19.66	0.71	1.61
3	99.15	35.27	5.00	6.29
4	127.90	43.60	2.10	4.03

It is noticeable from Tables II and III that the electrocatalytic activity of [α₁-LiP₂W₁₇O₆₁]⁹⁻ was greater than that of α₁-P₂W₁₇Cd in wave I, while this behavior was *vice versa* for wave II. This trend may be attributed to the presence of Cd²⁺. However, the electrocatalytic activity of [α₁-LiP₂W₁₇O₆₁]⁹⁻ decreased on cadmium ion substitution.

The inset of Fig. 9 presents four straight lines over a wide range of concentrations with different slopes, indicating that wave I had a higher catalytic activity than the other waves.

Electrocatalysis of NO_2^- reduction by $\alpha_2\text{-P}_2\text{W}_{17}\text{Cd}$

The polyoxometalates $[\alpha_2\text{-P}_2\text{W}_{17}\text{O}_{61}]^{10-}$ and $\alpha_2\text{-P}_2\text{W}_{17}\text{Cd}$ were tested at pH 4.7 for their activity in the reduction of nitrite ion. The CVs for the electrocatalytic reduction of NO_2^- by GC in 0.5 M acetate buffer solution are shown in Fig. 10.

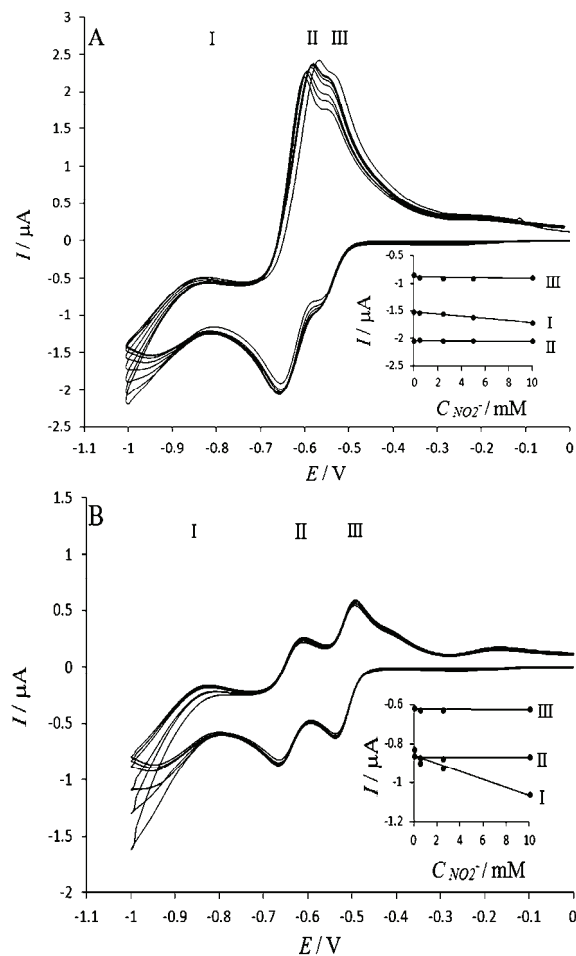


Fig. 10. A) Cyclic voltammograms (scan rate: 75 mV s⁻¹) for the electrocatalytic reduction of NO_2^- with a 5×10^{-4} M solution of $\alpha_2\text{-P}_2\text{W}_{17}\text{Cd}$ in a 0.5 M acetate buffer solution (from top to bottom $\gamma = 0, 1, 5, 10$ and 20). B) Cyclic voltammograms (scan rate: 75 mV s⁻¹) for the electrocatalytic reduction of NO_2^- with a 5×10^{-4} M solution of $\text{K}_{10}[\alpha_2\text{-P}_2\text{W}_{17}\text{O}_{61}]$ in a 0.5 M acetate buffer solution (from top to bottom $\gamma = 0, 1, 5$ and 20). The excess parameter defined as $\gamma = c_{(\text{NO}_2^-)}^0 / c_{(\text{POM})}^0$. Inset: the relationship between catalytic current and NO_2^- concentration.

Clearly, with the addition of NaNO_2 to the solution, even for small values of the excess parameter γ , cathodic current of all waves increased and the corresponding anodic current decreased. The catalytic efficiency *CAT* for wave I of $[\alpha_2\text{-P}_2\text{W}_{17}\text{O}_{61}]^{10-}$ varied from 8.34 to 28.17 % (Table IV) when $\gamma = 1, 5$ and 20, while the *CAT* variations for $\alpha_2\text{-P}_2\text{W}_{17}\text{Cd}$ were from 0.65 to 10.46 % when $\gamma = 1, 5, 10$ and 20 (Table V).

TABLE IV. Catalytic efficiency for $[\alpha_2\text{-P}_2\text{W}_{17}\text{O}_{61}]^{10-}$; $CATw_x$ refers to catalytic efficiency for the x^{th} wave

γ	$CATw_1 / \%$	$CATw_2 / \%$	$CATw_3 / \%$
1	8.34	1.27	1.45
5	11.60	1.74	1.94
20	28.17	0.69	0.97

TABLE V. Catalytic efficiency for $\alpha_2\text{-P}_2\text{W}_{17}\text{Cd}$; $CATw_x$ refers to catalytic efficiency for the x^{th} wave

γ	$CATw_1 / \%$	$CATw_2 / \%$	$CATw_3 / \%$
1	0.65	0.00	0.22
5	2.61	0.00	0.55
10	6.53	0.49	1.00
20	10.46	0.49	0.33

It is noticeable from Tables IV and V that the electrocatalytic activity of $[\alpha_2\text{-P}_2\text{W}_{17}\text{O}_{61}]^{10-}$ was greater than that of $\alpha_2\text{-P}_2\text{W}_{17}\text{Cd}$ in wave I, due to the presence of Cd^{2+} ion.

The inset of Fig. 10 presents four straight lines over a wide range of concentrations with different slopes, indicating that wave I had a higher catalytic activity than the other waves.

CONCLUSIONS

Two new cadmium-containing Wells–Dawson polyoxometalates were synthesized as water-soluble potassium salts. ^{113}Cd -NMR indicated that cadmium was substituted completely in the $[\alpha_2\text{-P}_2\text{W}_{17}\text{O}_{61}]^{10-}$ vacancy, whereas cadmium in $[\alpha_1\text{-LiP}_2\text{W}_{17}\text{O}_{61}]^{9-}$ did not fill completely the vacancy. Moreover, electrochemical investigations were in good agreement with this result because remarkable differences in the redox peaks were not observed between the $\alpha_1\text{-P}_2\text{W}_{17}\text{Cd}$ and $[\alpha_1\text{-LiP}_2\text{W}_{17}\text{O}_{61}]^{9-}$ compounds.

The electrochemistry of $\alpha_1\text{-P}_2\text{W}_{17}\text{Cd}$ and $\alpha_2\text{-P}_2\text{W}_{17}\text{Cd}$ was studied. First, these polyoxoanions exhibited four- and three-step redox waves attributed to the tungsten–oxo and cadmium–oxo redox processes in pH 4.7 solutions. The best electrocatalytic activity for $\alpha_1\text{-P}_2\text{W}_{17}\text{Cd}$ and $\alpha_2\text{-P}_2\text{W}_{17}\text{Cd}$ was observed in wave I, which is related to tungsten–oxo redox centers. In addition, decreases in the electrocatalytic activity of mono-lacunary Dawson-type ($[\alpha_1\text{-LiP}_2\text{W}_{17}\text{O}_{61}]^{9-}$ and $[\alpha_2\text{-P}_2\text{W}_{17}\text{O}_{61}]^{10-}$) follows from the presence of cadmium metal ion in these compounds. The presence of cadmium metal ion in the mono-lacunary Dawson-type ($[\alpha_1\text{-LiP}_2\text{W}_{17}\text{O}_{61}]^{9-}$ and $[\alpha_2\text{-P}_2\text{W}_{17}\text{O}_{61}]^{10-}$) caused decreases in electrocatalytic activity of these compounds.

ИЗВОД

СИНТЕЗА, КАРАКТЕРИЗАЦИЈА И УПОРЕЂИВАЊЕ ЕЛЕКТРОКАТАЛИТИЧКЕ
АКТИВНОСТИ ДВА МОНОЛАКУНАРНА WELLS–DAWSON ПОЛИОКСОМЕТАЛАТА
КОЈИ САДРЖЕ КАДМИЈУМ, α_1 -И α_2 -[$P_2W_{17}Cd(H_2O)O_{61}]^{8-}$

FARROKHZAD MOHAMMADI ZONOZ¹, ALI JAMSHIDI², FATEME HAJIZADEH¹ И KHADIJEH YOUSEFI³

¹Department of Chemistry, Hakim Sabzevari University, Sabzevar, 96179-76487, Iran, ²School of Chemistry, Damghan University, Damghan, Iran и ³Payamnoor University of Sari, Sari, Iran

У овом раду су синтетизоване калијумове соли два Wells–Dawson полиоксометалата који садрже кадмијум, $K_8[\alpha_1-P_2W_{17}Cd(H_2O)O_{61}] \cdot 14H_2O$ (α_1 - $P_2W_{17}Cd$) и $K_8[\alpha_2-P_2W_{17}Cd(H_2O)O_{61}] \cdot 16H_2O$ (α_2 - $P_2W_{17}Cd$). Синтетизовани комплекси су окарактерисани применом IR-, ³¹P- и ¹¹³Cd-NMR спектроскопије, док су редокс потенцијали волфрама и кадмијума у овим јединењима одређени применом цикличне волтаметрије (CV). Добијени резултати су показали да присуство јона кадмијума утиче на смањење електрокаталитичке активности $[\alpha_1-LiP_2W_{17}O_{61}]^{9-}$ и $\alpha_2-[P_2W_{17}O_{61}]^{10-}$ хетерополианјона.

(Примљено 18. јануара, ревидирано 18. маја, прихваћено 28. маја 2014)

REFERENCES

1. L. Ouahab, *Chem. Mater.* **9** (1997) 1909
2. M. T. Pope, A. Muller, *Angew. Chem. Int. Ed. Engl.* **30** (1991) 34
3. M. Witvrouw, H. Weigold, C. Pannecouque, D. Schols, E. D. Clercq, G. Holan, *J. Med. Chem.* **43** (2000) 77
4. C. L. Hill, R. B. Bown, *J. Am. Chem. Soc.* **108** (1986) 536
5. A. Watzenberger, G. Emig, D.T. Lynch, *J. Catal.* **124** (1990) 247
6. D. Mansuy, J. F. Bartoli, P. Battioni, D. K. Lyon, R. G. Finke, *J. Am. Chem. Soc.* **113** (1991) 7222
7. R. Contant, J.-P. Ciabrini, *J. Chem. Res. Synop.* **222** (1997) 2601
8. Z. Zhang, Y. Li, Y. Wang, Y. Qi, E. Wang, *Inorg. Chem.* **47** (2008) 7615
9. D. K. Lyon, W. K. Miller, T. Novet, P. J. Domaille, E. Evitt, D. C. Johnson, R. G. Finke, *J. Am. Chem. Soc.* **113** (1991) 7209
10. M. N. Sokolov, N. V. Izarova, E. V. Peresypkina, D. A. Mainichev, V. P. Fedin, *Inorg. Chim. Acta* **362** (2009) 3756
11. J. Choi, J. K. Kim, S. Park, J. H. Song, I. K. Song, *Appl. Catal. A*, **427–428** (2012) 84
12. G. Absillis, T. N. Parac-Vogt, *Inorg. Chem.* **51** (2012) 9902
13. S. Vanhaecht, G. Absillis, T. N. Parac-Vogt, *Dalton Trans.* **41** (2012) 10028
14. R. Contant, *J. Chem. Res., Synop.* (1984) 120
15. J. F. Kirby, L. C. V. Baker, *J. Am. Chem. Soc.* **117** (1995) 10010
16. L. H. Bi, E. B. Wang, J. Peng, R. D. Hung, L. Xu, C. W. Hu, *Inorg. Chem.* **39** (2000) 671
17. M. H. Alizadeh, H. Razavi, F. Mohammadi Zonozi, M. R. Mohammadi, *Polyhedron* **22** (2003) 933
18. F. Hussain, L. H. Bi, U. Rauwald, M. Reicke, U. Kortz, *Polyhedron* **24** (2005) 847
19. L. Chen, D. Shi, J. Zhao, Y. Wang, P. Ma, J. Wang, J. Niu, *Cryst. Growth Des.* **11** (2011) 1913
20. S. Q. Liu, D. Volkmer, D. G. Kurth, *J. Cluster Sci.* **14** (2003) 405
21. M. Green, J. Harries, G. Wakefield, R. Taylor, *J. Am. Chem. Soc.* **127** (2005) 12812
22. L. Cheng, J. A. Cox, *Electrochim. Commun.* **3** (2001) 285
23. G. G. Gao, L. Xu, W. J. Wang, W. J. An, Y. F. Qiu, Z. Q. Wang, E. B. Wang, *J. Phys. Chem., B* **109** (2005) 8948

24. J. Y. Qu, X. Q. Zou, B. F. Liu, S. J. Dong, *Anal. Chim. Acta* **599** (2007) 51
25. A. Kuhn, F. C. Anson, *Langmuir* **12** (1996) 5481
26. X. Xi, S. Dong, *J. Mol. Catal., A* **114** (1996) 257
27. W. R. Epperly, *Chemtech* (1991) 429
28. R. Contant, *Inorg. Synth.* **27** (1990) 104
29. Y. Saku, Y. Sakai, K. Noniya, *Inorg. Chim. Acta* **363** (2010) 967
30. I. M. Mbomekalle, Y. W. Lu, B. Keita, L. Nadjo, *Inorg. Chem. Commun.* **7** (2004) 86
31. K. Kim, M. T. Pope, G. J. Gama, M. H. Dickman, *J. Am. Chem. Soc.* **32** (1976) 11164
32. R. Contant, M. Abbessi, J. C. A. Belhouari, B. Keita, L. Nadjo, *Inorg. Chem.* **36** (1997) 4961
33. J. Bartis, Y. Kunina, M. Blumenstein, L. C. Francesconi, *Inorg. Chem.* **35** (1996) 1497
34. J. Bartis, M. Dankova, J. J. Lessmann, Q. Luo, W. Horrocks, L. C. Francesconi, *Inorg. Chem.* **38** (1999) 1042
35. D. McGregor, B. P. Burton-Pye, R. C. Howell, I. M. Mbomekalle, W. W. Lukens Jr., F. Bian, E. Mausolf, F. Poineau, K. R. Czerwinski, L. C. Francesconi, *Inorg. Chem.* **50** (2011) 1670
36. www.csudh.edu, <http://www.csudh.edu/oliver/chemdata/data-e.htm> (18/01/2014)
37. M. T. Pope, A. Muller, E. Papaconstantinou, A. Ioannidis, A. Hiskia, P. Argitis, D. Dimoticali, S. Korres, *Polyoxometalates: from Platonic Solids to Antiretroviral Activity*, Kluwer, Dordrecht, 1994, p. 327
38. B. Keita, E. Abdeljalil, L. Nadjo, R. Contant, R. Belgiche, *Electrochim. Commun.* **3** (2001) 56
39. B. Keita, I. Mbomekalle, L. Nadjo, P. Oliveira, A. Ranjbari, R. Contant, *C. R. Chim.* **8** (2005) 1057.